

**You might find this additional information useful...**

---

This article cites 41 articles, 25 of which you can access free at:

<http://jn.physiology.org/cgi/content/full/95/5/3235#BIBL>

This article has been cited by 3 other HighWire hosted articles:

**Glutamatergic Inputs Contribute to Phasic Activity in Vasopressin Neurons**

J.-M. Israel, D. A. Poulain and S. H. R. Oliet  
*J. Neurosci.*, January 27, 2010; 30 (4): 1221-1232.  
[\[Abstract\]](#) [\[Full Text\]](#) [\[PDF\]](#)

**Dehydration-induced modulation of  $\mu$ -opioid inhibition of vasopressin neurone activity**

V. Scott, V. R. Bishop, G. Leng and C. H. Brown  
*J. Physiol.*, December 1, 2009; 587 (23): 5679-5689.  
[\[Abstract\]](#) [\[Full Text\]](#) [\[PDF\]](#)

**Feedback inhibition of action potential discharge by endogenous adenosine enhancement of the medium afterhyperpolarization**

M. Ruan and C. H. Brown  
*J. Physiol.*, March 1, 2009; 587 (5): 1043-1056.  
[\[Abstract\]](#) [\[Full Text\]](#) [\[PDF\]](#)

Updated information and services including high-resolution figures, can be found at:

<http://jn.physiology.org/cgi/content/full/95/5/3235>

Additional material and information about *Journal of Neurophysiology* can be found at:

<http://www.the-aps.org/publications/jn>

---

This information is current as of February 10, 2010 .

# Endogenous Activation of Supraoptic Nucleus $\kappa$ -Opioid Receptors Terminates Spontaneous Phasic Bursts in Rat Magnocellular Neurosecretory Cells

Colin H. Brown,<sup>1,2,3</sup> Gareth Leng,<sup>2</sup> Mike Ludwig,<sup>2</sup> and Charles W. Bourque<sup>3</sup>

<sup>1</sup>Centre for Neuroendocrinology and Department of Physiology, School of Medical Sciences, University of Otago, Dunedin, New Zealand; <sup>2</sup>Centre for Integrative Physiology, University of Edinburgh, Edinburgh United Kingdom; and <sup>3</sup>Centre for Research in Neuroscience, Montreal General Hospital and McGill University, Montreal, Quebec, Canada

Submitted 19 January 2006; accepted in final form 15 February 2006

**Brown, Colin H., Gareth Leng, Mike Ludwig, and Charles W. Bourque.** Endogenous activation of supraoptic nucleus  $\kappa$ -opioid receptors terminates spontaneous phasic bursts in rat magnocellular neurosecretory cells. *J Neurophysiol* 95: 3235–3244, 2006. First published February 22, 2006; doi:10.1152/jn.00062.2006. Phasic activity in magnocellular neurosecretory vasopressin cells is characterized by alternating periods of activity (bursts) and silence. During phasic bursts, action potentials (spikes) are superimposed on plateau potentials that are generated by summation of depolarizing afterpotentials (DAPs). Burst termination is believed to result from autocrine feedback inhibition of plateau potentials by the  $\kappa$ -opioid peptide, dynorphin, which is copackaged in vasopressin neurosecretory vesicles and exocytosed from vasopressin cell dendrites during phasic bursts. Here we tested this hypothesis, using intracellular recording in vitro to show that  $\kappa$ -opioid receptor antagonist administration enhanced plateau potential amplitude to increase postspike excitability during spontaneous phasic activity. The antagonist also increased postburst DAP amplitude in vitro, indicating that endogenous dynorphin probably reduces plateau potential amplitude by inhibiting the DAP mechanism. However, the  $\kappa$ -opioid receptor antagonist did not affect the slow depolarization that follows burst termination, suggesting that recovery from endogenous  $\kappa$ -opioid inhibition does not contribute to the slow depolarization. We also show, by extracellular single-unit recording, that there is a strong random element in the timing of burst initiation and termination in vivo. Administration of a  $\kappa$ -opioid receptor antagonist eliminated the random element of burst termination but did not alter the timing of burst initiation. We conclude that dendritic dynorphin release terminates phasic bursts by reducing the amplitude of plateau potentials to reduce the probability of spike firing as bursts progress. By contrast, dendritic dynorphin release does not greatly influence the membrane potential between bursts and evidently does not influence the timing of burst initiation.

## INTRODUCTION

Phasic activity in magnocellular neurosecretory cells (MNCs) of the hypothalamic supraoptic nucleus (SON) and paraventricular nucleus is characterized by action potential (spike) discharge in periods of firing (bursts) that each last tens of seconds, separated by silent periods (interburst intervals) of similar duration; this pattern is highly efficient for secretion of vasopressin (the antidiuretic hormone) into the circulatory system (Leng et al. 1999). Bursts are sustained by plateau potentials that are generated by temporal summation of non-synaptic depolarizing afterpotentials (DAPs) that follow each spike (Andrew and Dudek 1983; Armstrong et al. 1994;

Ghamari-Langroudi and Bourque 1998; Li et al. 1995; Li and Hatton 1997). The best-characterized mechanism for burst termination is via autocrine feedback inhibition of DAPs by the  $\kappa$ -opioid peptide, dynorphin (Brown and Bourque 2004). Dynorphin is copackaged with vasopressin and  $\kappa$ -opioid receptors in neurosecretory vesicles (Shuster et al. 2000) that are exocytosed from the dendrites (as well as the terminals) of SON cells (Pow and Morris 1989).

The synthetic  $\kappa$ -opioid receptor agonist, U50,488H, and endogenous dynorphin both inhibit DAPs and decrease burst duration in vitro (Brown and Bourque 2004; Brown et al. 1999). Thus it has been hypothesized that endogenous dynorphin terminates bursts by autocrine feedback inhibition of the plateau potential (Brown 2004; Brown and Bourque 2006). Furthermore, mathematical modeling of phasic activity in vitro has indicated that endogenous dynorphin might also be involved in the timing of burst initiation (Roper et al. 2004). Therefore autocrine feedback inhibition of DAPs appears to be essential for phasic activity in vasopressin MNCs, and indeed, desensitization of SON  $\kappa$ -opioid receptors virtually eliminates phasic activity in MNCs in vivo (Brown et al. 1998). However, phasic firing is not regenerative in vivo (Brown et al. 2004a) and so the contribution of plateau potential inhibition to autocrine  $\kappa$ -opioid inhibition of phasic bursts is less clear in vivo.

Here, we characterized the effects of endogenous dynorphin on membrane potential during spontaneous phasic activity in vitro and on the rhythmicity of phasic MNCs in vivo to determine whether the changes induced in membrane potential in vitro are consistent with the observed changes in phasic patterning in vivo. First, by in vitro intracellular recording we show that endogenous dynorphin decreases plateau potential amplitude during spontaneous phasic activity to reduce the probability of spike firing, but does not alter interburst membrane potential. We then analyzed burst durations and interburst intervals from recordings of spontaneous phasic activity in vivo to show that endogenous dynorphin increases the probability of burst termination, but does not influence the timing of burst initiation, as would be expected from the effects of dynorphin in vitro.

## METHODS

### *In vitro electrophysiology*

In a procedure approved by the McGill University Animal Care Committee, conscious male Long–Evans rats (approximately 150–250 g)

Address for reprint requests and other correspondence: Dr Colin H. Brown, Centre for Neuroendocrinology and Department of Physiology, School of Medical Sciences, University of Otago, P.O. Box 913, Dunedin, New Zealand. (E-mail: colin.brown@stonebow.otago.ac.nz)

The costs of publication of this article were defrayed in part by the payment of page charges. The article must therefore be hereby marked “advertisement” in accordance with 18 U.S.C. Section 1734 solely to indicate this fact.

were restrained in a soft plastic cone (5–10 s) and decapitated, and their brains were rapidly removed. A block of tissue 8 x 8 x 2 mm containing the basal hypothalamus was excised using razor blades and pinned, ventral surface up, to the Sylgard base of a superfusion chamber. Within 2–3 min, the excised hypothalamic explant was superfused (at 0.5–1.0 ml min<sup>-1</sup> at 32–33°C) with carbogenated (95% O<sub>2</sub>-5%CO<sub>2</sub>) artificial CSF (aCSF; see following text) delivered via a Tygon tube placed over the medial tuberal region. The arachnoid membrane overlying the SON was removed using fine forceps, and a cotton wick was placed at the rostral tip of the explant to facilitate aCSF drainage.

Intracellular recordings were made using sharp micropipettes prepared from glass capillaries (1.2 mm O.D.; AM Systems, Everett, WA) pulled on a P-87 Flaming-Brown puller (Sutter Instruments, Novato, CA). Micropipettes were filled with 2 M potassium acetate to yield DC resistances of 70–160 MΩ to an Ag-AgCl wire electrode immersed in aCSF. Voltage recordings (DC–3 kHz) were obtained using an Axoclamp 2A amplifier (Axon Instruments, Foster City, CA) in continuous current-clamp (“bridge”) mode. Acquired signals were displayed on a chart recorder and digitized (44 kHz; Neurodata, Delaware Water Gap, PA) for storage on videotape. For analyses, signals were digitized (5 or 10 kHz; DigiData 1200 Interface, Axon Instruments), stored on a personal computer running Clampex (Axon Instruments), and analyzed off-line using Clampfit (Axon Instruments). Current pulses were delivered by a Digitimer DS2 isolated stimulator (Welwyn, Garden City, UK) connected to a pulse generator (Digitimer D-4030). Recordings were made from SON cells impaled with sharp electrodes in superfused hypothalamic explants. The cells had resting membrane potentials more negative than –50 mV, input resistances of >150 MΩ, and spike amplitudes of >60 mV when measured from baseline. Each cell displayed frequency-dependent spike broadening and transient outward rectification when depolarized from initial membrane potentials more negative than –75 mV (characteristics specific to SON cells (Renaud and Bourque 1991)) and exhibited spontaneous phasic activity.

The aCSF (pH 7.4; 295 ± 3 mOsmol kg<sup>-1</sup>) was composed of (in mM): 120 NaCl, 3 KCl, 1.2 MgCl<sub>2</sub>, 26 NaHCO<sub>3</sub>, 2.5 CaCl<sub>2</sub>, and 10 glucose (Fisher Scientific, Pittsburgh, PA). One hundred micromolars of the κ-opioid receptor antagonist, *nor*-binaltorphimine (BNI; Tocris Cookson, Ballwin, MO), was prepared in deionized water, stored frozen until the day of use, and bath applied after dilution to 1 μM in aCSF.

### *In vitro* electrophysiology data analysis

Spikes were identified during spontaneous phasic bursts using the threshold search function on Clampex. Membrane potential was monitored during each burst as the mean membrane potential measured between 97.5 and 102.5 ms after the peak of each spike (where a second spike did not fire within 110 ms of the preceding spike). This postspike interval was selected for analysis to allow for full recovery of membrane potential from the postspike fast after-hyperpolarization (AHP), which has a time constant of <20 ms (Bourque et al. 1985), without excessive elimination of data due to the occurrence of the subsequent spike (i.e., >95% of spikes recorded under control conditions were included in the analyses using this time period, whereas only 77% of spikes would be included in analyses at 200 ms after each spike, with particularly high drop-out early in bursts, where firing rate is typically higher; Kirkpatrick and Bourque 1996). Plateau potential amplitude was calculated by subtracting the mean membrane potential measured over >1 s during the preceding interburst interval (where the current injection was the same as during the burst).

The probability of spike firing (hazard) was calculated from the interspike interval histogram of individual cells using the formula

$$h_{[i-1, i]} = n_{[i-1, i]} / (N - n_{[0, i-1]})$$

where  $h_{[i-1, i]}$  is the hazard at interval  $i$ ,  $n_{[i-1, i]}$  is the number of spikes in interval  $i$ ,  $n_{[0, i-1]}$  is the total number of spikes preceding the current

interval, and  $N$  is the total number of spikes in all intervals. This gives the inferred probability (as a decimal) of a cell firing a subsequent spike in any interval after a spike (at *time 0*), given that another spike has not occurred earlier.

The final spike in each spontaneous burst was identified using the threshold search function on Clampex, and segments of recording starting 0.2 s before, and lasting 30 s after, the peak of the final spike were saved (to avoid the confounding effects of individual spikes, and of the onset of subsequent burst, on membrane potential over the period when most [62–79% in the current study] spontaneous bursts start *in vivo*). Only periods of recording during which no further spikes occurred and no adjustments were made to the current injection were used for the analyses (21 bursts under basal conditions and 16 bursts in BNI, both from four cells; two of the four cells eventually adopted continuous activity in the continued presence of BNI and only bursts prior to this point were used in the analyses). The baseline of each segment of recording was adjusted to spike threshold of the final spike (2 mV ms<sup>-1</sup> increase in membrane potential), and the peak of the postspike DAP was measured relative to spike threshold. The post-burst membrane potential was averaged for each cell in each condition using Clampex. The averaged “cell” postburst membrane potentials were then averaged using Clampex to generate the “group” postburst membrane potentials for each condition.

### *In vivo* electrophysiology

Because of the difficulty in maintaining stable recording of phasic activity for sufficient periods to allow comprehensive analysis of the distribution of spontaneous burst onset and termination (>1 h) *in vitro*, we used extracellular single-unit *in vivo* to investigate these parameters.

All *in vivo* electrophysiological procedures were carried out in accordance with the UK Animals (Scientific Procedures) Act 1986 and associated guidelines. Female Sprague–Dawley rats (250–300 g;  $n = 33$ ) were anesthetized by intraperitoneal injection of urethane (ethyl carbamate; 1.25 g kg<sup>-1</sup>), and a catheter was inserted into the left femoral vein for drug injection. The pituitary stalk and right SON were exposed through the oral cavity. For six experiments, an in-house designed U-shaped microdialysis probe (total membrane length 2.0 mm; Spectra/Por RC Hollow Fibers, Spectrum Med. Inc., Houston, TX) was bent to position the loop of the membrane flat onto the exposed ventral surface of the brain over the SON (after removal of the meninges) for microdialysis application of BNI. Extracellular single-unit recordings were made using a glass recording microelectrode (15–40 MΩ; placed in the caudal SON, through the center of the dialysis loop, when present) and conventional electrophysiological recording techniques (Ludwig and Leng 1997). A side-by-side stimulating electrode (Clark Electromedical Instruments, Pangbourne, Reading, UK) was placed on the pituitary stalk to elicit antidromic spikes in SON cells. Antidromically identified neurons were confirmed as SON cells by collision of antidromic spikes by spontaneous orthodromic spikes (Lincoln and Wakerley 1974). Where BNI was administered (0.2 μg μl<sup>-1</sup> at 2 μl min<sup>-1</sup> for >30 min), the SON was dialyzed with aCSF (pH 7.2, composition in mM: 138 NaCl, 3.36 KCl, 9.52 NaHCO<sub>3</sub>, 0.49 Na<sub>2</sub>HPO<sub>4</sub>, 2.16 urea, 1.26 CaCl<sub>2</sub>, 1.18 MgCl<sub>2</sub>) at 2 μl min<sup>-1</sup> before recording. At the end of experiments, the rats were killed by intravenous anesthetic overdose (60 mg kg<sup>-1</sup> pentobarbital). For microdialysis application, BNI (Tocris Cookson, Avonmouth, Bristol, UK) was dissolved in aCSF at the final required concentration and stored frozen in aliquots until the day of use.

### *In vivo* electrophysiology data analysis

SON cell activity was recorded onto computer and analyzed off-line using Spike2 software (Cambridge Electronic Design, Cambridge, UK). Bursts were characterized using the “bursts” script in Spike2; spontaneous bursts were defined as activity lasting >5 s,

containing >20 spikes, and including a >5-s interval between bursts during which there was <1 spike every 5 s (Brown et al. 1998). For each condition, periods of stable activity lasting 300–900 s were selected for analysis. Such analyses partitioned more than 95% of recorded spikes into bursts. A total of 534 bursts were analyzed from 34 SON cells (4–53 bursts per cell).

The probabilities of burst termination and initiation and of single spikes occurring between bursts were also calculated from the distribution histograms of each of these events using the formula

$$h_{[i-1, i]} = n_{[i-1, i]} / (N - n_{[0, i-1]})$$

and (because the hazard at any given time is a proportion), the confidence interval of the hazard was calculated using the formula

$$CI_{[i-1, i]} = \sqrt{(h_{[i-1, i]}(1 - h_{[i-1, i]})(N - n_{[0, i-1]})}$$

where  $h_{[i-1, i]}$  is the hazard of burst termination (or burst initiation, or a single spike firing after the end of the preceding burst) in interval  $i$ ,  $n_{[i-1, i]}$  is the number of burst terminations (or burst initiations, or single spikes firing after the end of the preceding burst) in interval  $i$ ,

$n_{[0, i-1]}$  is the total number of burst terminations (or burst initiations, or single spikes firing after the end of the preceding burst) preceding the current interval,  $N$  is the total number of burst terminations (or burst initiations, or single spikes firing after the end of the preceding burst) in all intervals, and  $CI_{[i-1, i]}$  is the confidence interval of the hazard in interval  $i$ .

Statistics

All statistical comparisons and regressions were completed using SigmaStat software (SPSS Science, Chicago, IL). Analyses were considered statistically significant at  $P \leq 0.05$ . Nonlinear regressions were fitted using the Marquardt–Levenberg algorithm to calculate the parameters that minimize the sum of the squared differences between the observed and predicted values of the dependent variable (hazard). Where multiple observations were used from individual cells, unpaired statistical comparisons were applied, and where averaged values were used from individual cells, paired comparisons were applied.

RESULTS

Plateau potential amplitude during spontaneous phasic bursts in vitro

We have previously shown that BNI increases burst duration in vitro (Brown and Bourque 2004). To test whether this results from effects on the plateau potential, we recorded the membrane potential from eight SON cells in hypothalamic explants during spontaneous phasic activity (e.g., Fig. 1A–C). We analyzed 7,833 spikes from 115 bursts; 1,215 (15.5%) of plateau potential measurements were eliminated because a subsequent spike fired within 110 ms of the spike under analysis, 4.4% of spikes were eliminated under control conditions, and 24.0% were eliminated in the presence of BNI (because of the faster firing rate in BNI).

Under basal conditions, the mean ( $\pm$ SE) plateau potential amplitude after the first spike of bursts was  $2.1 \pm 0.3$  mV and remained approximately the same (between 1.3 and 2.4 mV)

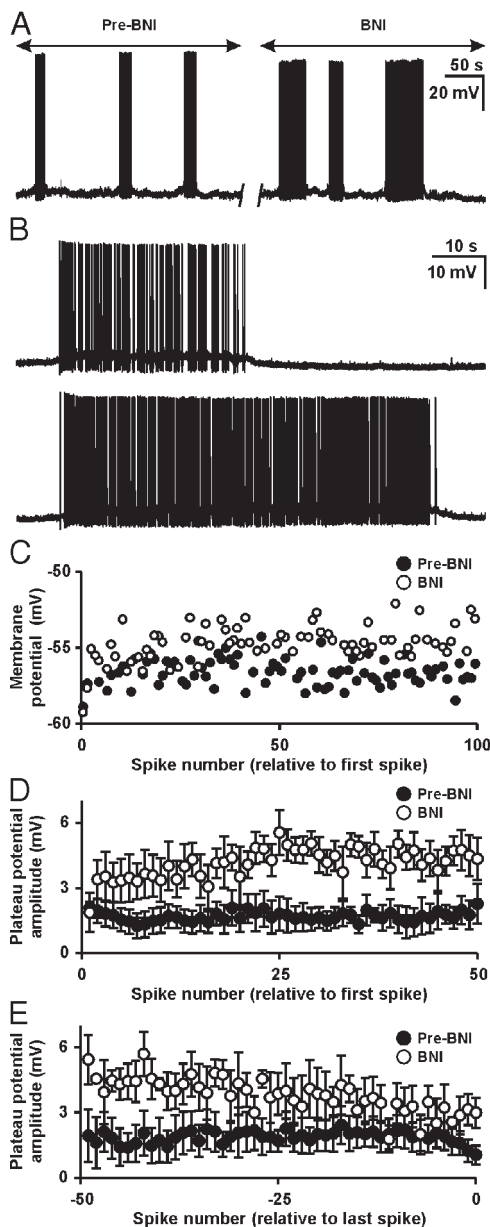


FIG. 1. Endogenous κ-opioid peptides reduce plateau potential amplitude in vitro. *A*: current-clamp recording of the membrane potential of a supraoptic nucleus (SON) cell during spontaneous phasic activity, before (*left*) and during (*right*) superfusion of 1 μM nor-binaltorphimine (BNI). Note that BNI increased the duration of spontaneous phasic bursts, typical of all cells tested (Brown and Bourque 2004). *B*: SON cell (a different cell from that shown in *A*) membrane potential during individual spontaneous bursts, before (*top*) and during (*bottom*) superfusion of 1 μM BNI. *C*: mean membrane potential measured 97.5–102.5 ms after the first 100 spikes of the bursts from *B* (measurements made following spikes after which another spike fired within 110 ms were excluded) before (filled circles) and during (open circles) BNI superfusion, showing the temporal profile of the evolution of the plateau potential under control conditions (6 of 8 cells showed a subjectively similar profile) and that BNI increased the steady-state depolarization during the plateau potential. *D*: plateau potential amplitude (relative to preburst membrane potential) over the first 50 spikes of spontaneous bursts before (filled circles) and during (open circles) BNI superfusion. Note that, because of differences in DAP summation and spike frequency adaptation between cells at the beginning of bursts, the maximum mean plateau potential amplitude appears early in bursts under control conditions. Nevertheless, in the presence of BNI, the plateau potential increases over the first 25 spikes of bursts, indicating a progressive κ-opioid inhibition of plateau potential amplitude under basal conditions. *E*: plateau potential amplitude over the last 50 spikes of spontaneous bursts before (filled circles) and during (open circles) BNI superfusion, showing that plateau potential amplitude is maintained until the last few spikes of a burst under control conditions, whereas during BNI superfusion, plateau potential amplitude declines steadily over the last 20–30 spikes of bursts.

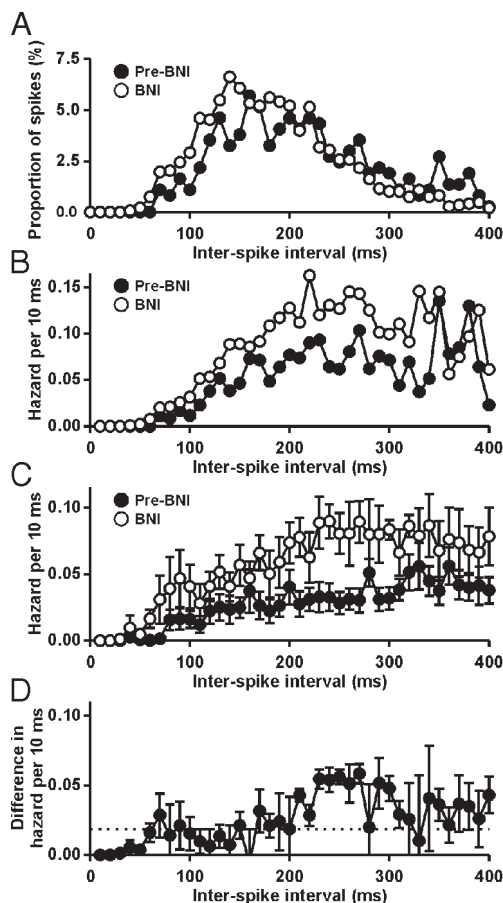


FIG. 2. Endogenous  $\kappa$ -opioid peptides reduce postspike excitability during phasic bursts in vitro. *A*: interspike interval histogram of a phasic SON cell before (filled circles) and during (open circles) superfusion of  $1 \mu\text{M}$  BNI. *B*: hazard functions calculated from the interspike interval histograms in *A*, showing that BNI (open circles) increased the probability of spike firing (hazard) after each spike. *C*: mean hazard function before (filled circles) and during (open circles) BNI superfusion, showing that the BNI-induced increase in the probability of spike firing was consistent among all SON cells tested. *D*: subtraction plot of the difference in hazard before and during BNI superfusion, showing that the BNI-induced increase in the probability of spike firing was most prominent in the period approximately 200–300 ms after each spike. The dashed line shows the 95% confidence interval of the difference in hazard plotted against the *x*-axis to illustrate the separation of the BNI-sensitive hazard from zero.

for the remainder of the bursts (Fig. 1, *D* and *E*), until the last five spikes of bursts, when plateau potential amplitude progressively declined to  $1.0 \pm 0.4$  mV after the final spike of bursts (Fig. 1*E*).

In the presence of BNI, the amplitude of the plateau potential after the first spike was similar to that under basal conditions ( $1.8 \pm 0.9$  mV;  $P = 0.76$  vs. basal, Student's *t* test; Fig. 1, *C* and *D*) but thereafter increased progressively to a maximum of  $5.6 \pm 1.0$  mV after 25 spikes (Fig. 1*D*), indicating that activity-dependent release of an endogenous  $\kappa$ -opioid agonist restrains plateau potential amplitude over the course of spontaneous bursts. In the continued presence of BNI, plateau potential amplitude declined progressively over the last 50 spikes of bursts (Fig. 1*E*). Nevertheless, plateau potential amplitude after the final spike of spontaneous bursts was higher in the presence of BNI ( $3.0 \pm 0.9$  mV) than under basal conditions ( $P = 0.03$  vs. basal, Student's *t* test), indicating that a mechanism other than

plateau potential inhibition must terminate firing during  $\kappa$ -opioid receptor blockade.

#### Postspike excitability during spontaneous phasic bursts in vitro

BNI increases postspike excitability during phasic bursts in vivo, and this has been inferred to reflect changes in the postspike potentials that underpin the plateau potential (Brown et al. 2004b). Accordingly, we calculated the postspike excitability of SON cells during spontaneous phasic bursts in vitro. Similar to previous analysis (Sabatier et al. 2004), all of these cells had interspike interval distributions with modes of  $>150$  ms (e.g., Fig. 2*A*). The postspike excitability of SON cells is more clearly exposed by plots of the hazard function (Brown and Leng 2000), which reflects the changes in excitability of neurons after spontaneous spikes by displaying the inferred probability of spike firing with time after the preceding spike (Fig. 2, *B* and *C*). BNI increased the postspike excitability across a wide range of interspike intervals (Fig. 2*C*), but this increase was most pronounced between 200 and 300 ms after each spike (Fig. 2*D*), at a time when the postspike DAP is maximal in vitro (Brown and Bourque 2004). Thus BNI prolongs spontaneous phasic bursts by an increase in postspike excitability, which probably involves release (disinhibition) of the DAP mechanism from endogenous  $\kappa$ -opioid inhibition.

#### Effects of $\kappa$ -opioid receptor antagonism on interburst membrane potential

As it has been proposed that clearance of endogenous dynorphin contributes to the generation of the interburst interval (Roper et al. 2004), we next determined whether BNI altered the postburst membrane potential. BNI increased the postburst DAP ( $P = 0.04$ ) but did not alter the time course of the slow depolarization that follows phasic bursts in vitro (Fig. 3). Under basal conditions, the minimum value of the averaged interburst membrane potential was 10.6 mV below spike threshold at 4.1 s after the last spike; thereafter, a slow depolarization was fit by a linear regression,  $V_m = -10.983 + 0.399t$  ( $R^2 = 0.99$ ,  $P < 0.001$ ), where  $V_m$  = membrane potential and  $t$  = time from minimum  $V_m$ , giving a rate of  $0.40$  mV  $s^{-1}$  for the evolution of the slow depolarization. In the presence of BNI, the minimum interburst membrane potential was 11.2 mV below threshold at 4.2 s after the last spike, and the slow depolarization was fit by a linear regression,  $V_m = -11.305 + 0.442t$  ( $R^2 = 0.99$ ,  $P < 0.001$ ), giving a rate of  $0.44$  mV  $s^{-1}$  for the evolution of the slow depolarization in BNI. The resulting averaged membrane potential for each of the four cells at the end of the analysis period was similar ( $P = 0.24$ , paired *t* test) before and during BNI administration at  $-0.6 \pm 0.2$  mV and  $+0.4 \pm 0.7$  mV (relative to spike threshold of the last spike of the preceding burst), respectively.

For these four cells, the mean burst duration was  $10.7 \pm 1.6$  s ( $n = 48$  bursts from four cells) and  $48.2 \pm 7.0$  s ( $n = 23$  bursts from four cells) before and during BNI administration ( $P < 0.0001$ , Student's *t* test), and the mean interburst interval was  $56.4 \pm 8.8$  s and  $66.3 \pm 7.7$  s before and during BNI administration ( $P = 0.53$ , Student's *t* test). Two of these four

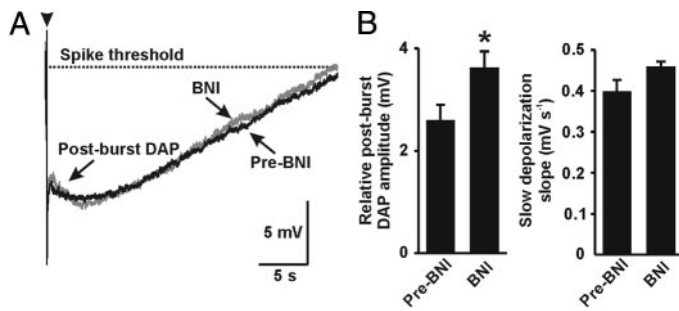


FIG. 3. Endogenous  $\kappa$ -opioid peptides do not modulate the interburst slow depolarization. *A*: membrane potential from 0.2 s before until 30 s after the last spike of spontaneous bursts (arrowhead, spike truncated) before (black; averaged after 21 bursts from 4 cells) and during (gray; averaged after 16 bursts from 4 cells) BNI superfusion; the postburst membrane potential was averaged for the bursts from each cell before and during BNI, and then these “cell averages” were averaged across cells to generate the traces as shown. Note the presence of a postburst depolarizing after-potential (DAP) that is enhanced in the presence of BNI and a slow depolarization that is unaffected by BNI. *B*: mean postburst DAP amplitudes (from individual bursts and arbitrarily represented as a positive measurement from 10 mV below spike threshold) before (pre-BNI;  $n = 21$  DAPs from four cells) and during ( $n = 16$  DAPs from four cells) BNI superfusion ( $*P < 0.05$ , Student’s  $t$ -test). *C*: slope of the slow depolarization (averaged for each cell in pClamp) before (pre-BNI) and during BNI superfusion ( $P = 0.12$ , paired  $t$ -test;  $n = 4$ ).

cells eventually adopted continuous activity (i.e., activity was artificially terminated by hyperpolarizing current injection) in the continued presence of BNI; only bursts prior to this point were used in the preceding analyses. It should also be noted that to maintain recordings of phasic activity over prolonged periods, current injection is frequently adjusted in the interburst interval to maintain baseline membrane potential and that the measured interburst intervals are confounded by such adjustments. Hence, we used *in vivo* extracellular single-unit recordings to analyze the distribution of burst durations and interburst intervals.

*Distributions of burst durations during spontaneous activity in vivo*

To determine the whether the changes in plateau potentials and postspike excitability induced by BNI (identified *in vitro*) were translated into changes in burst patterning *in vivo*, the distributions of burst duration and interburst interval were calculated (in 5-s intervals) from extracellular recordings of 324 bursts from 28 SON cells (4–28 bursts from each cell) that displayed spontaneous phasic activity *in vivo* (e.g., Fig. 4*A*).

Under basal conditions, the distribution of burst durations was highly skewed ( $P < 0.0001$ , Kolmogorov-Smirnov nor-

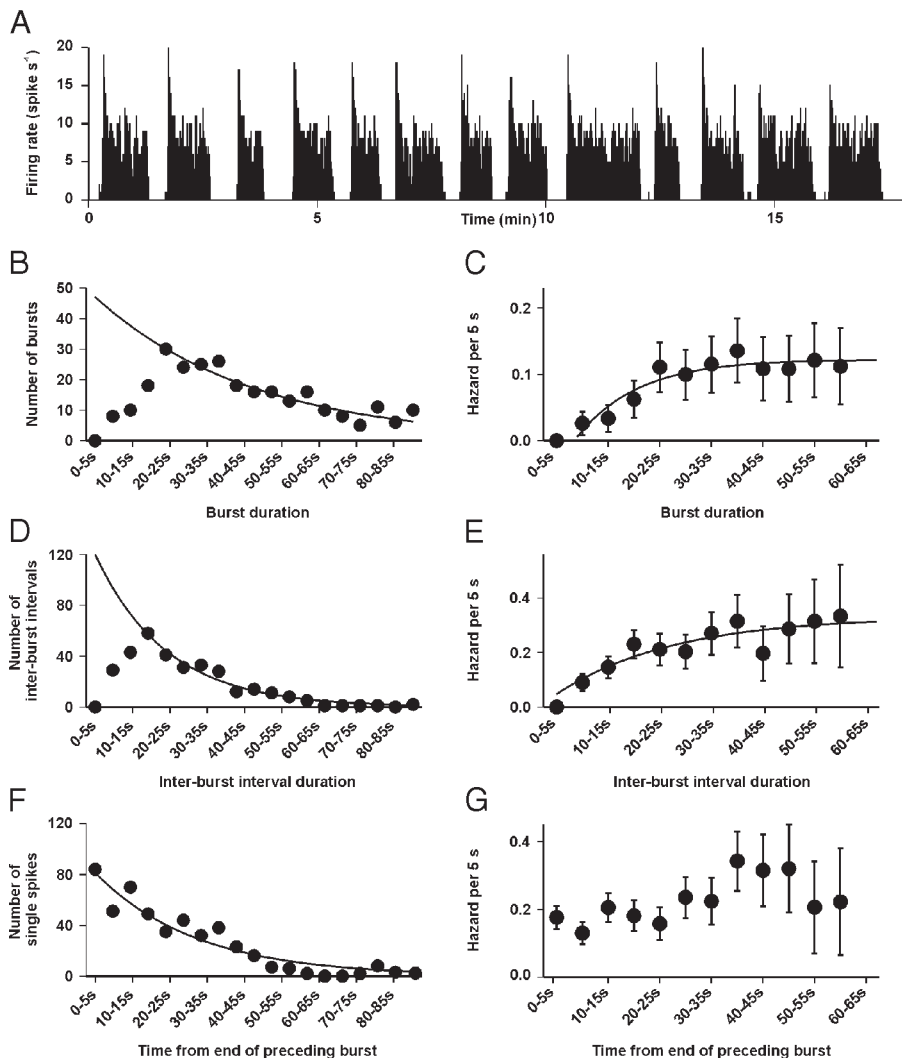


FIG. 4. Distributions of burst duration, interburst intervals, and single spikes between bursts *in vivo*. *A*: ratemeter record of an extracellular single-unit recording of the firing rate (in 1-s bins) of a spontaneously phasic SON cell in a urethane-anesthetized rat. Note the clear periods of activity (bursts), separated by silent periods (interburst intervals), and the profound spike frequency adaptation (reduction in firing rate over the course of bursts), typical of phasic activity in vasopressin cells. *B*: distribution of burst durations under basal conditions (324 bursts from 28 SON cells); the tail of the histogram is fit by a single exponential decay:  $f(t) = 47.111 \exp(-0.0224t)$ , where  $t =$  time (burst duration);  $R^2 = 0.90$ ,  $P < 0.001$ . *C*: hazard function generated from the burst distribution in *B* ( $\pm 95\%$  confidence interval), fit by single exponential rise to maximum:  $f(t) = 0.163 [1 - \exp(-0.0835t)] - 0.0405$  ( $R^2 = 0.64$ ,  $P < 0.001$ ). Note that the probability of burst termination increased to a maximum after 20–25 s under basal conditions. *D*: distribution of interburst intervals under basal conditions; the tail of the histogram is fit by a single exponential decay:  $f(t) = 20.080 \exp(-0.0498t)$ , where  $t$  is time (interburst interval);  $R^2 = 0.96$ ,  $P < 0.001$ . *E*: hazard function generated from the interburst interval distribution in *D* ( $\pm 95\%$  confidence interval), fit by single exponential rise to maximum:  $f(t) = 0.285 [1 - \exp(-0.044t)] + 0.047$ , where  $t$  is interburst interval;  $R^2 = 0.78$ ,  $P = 0.001$ . Because relatively few intervals ( $<5\%$ ) were  $>60$  s, only the hazard from intervals  $<60$  s are plotted. *F*: distribution of single spikes between bursts (relative to the end of the preceding burst) under basal conditions; the histogram is fit by a single exponential decay:  $f(t) = 81.472 \exp(-0.035t)$ , where  $t$  is time (from the end of the previous burst);  $R^2 = 0.90$ ,  $P < 0.001$ . *G*: hazard function generated from the single spike distributions in *F* ( $\pm 95\%$  confidence interval).

ality test), and only 11.1% of durations were shorter than the mode (20–25 s, mean  $58.7 \pm 3.3$  s, median 45.4 s,  $n = 324$  bursts from 28 cells). The tail of the histogram was fit well by a single negative exponential decay ( $R^2 = 0.90$ ,  $P < 0.001$ , Fig. 4B):  $f(t) = 47.111 \exp(-0.0224t)$ , where  $t =$  time (burst duration). Events that arise as a result of a Poisson process generate interval distributions that can be described by a single negative exponential, so this shape of burst duration distribution is consistent with the interpretation that burst termination occurs randomly after 20–25 s of burst firing.

The probability of burst termination at any given time during a burst is more clearly exposed by plots of the hazard function of burst duration; under basal conditions, the hazard function of burst duration ( $t$ ) was fit by a single exponential rise to a maximum ( $R^2 = 0.64$ ,  $P < 0.001$ , Fig. 4C):  $f(t) = 0.163 [1 - \exp(-0.0835t)] - 0.0405$ , indicating that the probability of burst termination increased over the first 20–25 s of burst firing and remained relatively constant thereafter.

Because endogenous  $\kappa$ -opioid receptor activation decreases burst duration in vivo (Brown et al. 1998 2004b) and in vitro (Brown and Bourque 2004), we tested whether burst duration was affected by pharmacological blockade of  $\kappa$ -opioid receptors in six cells by microdialysis application of BNI directly into the SON. As previously reported (Brown et al. 1998 2004b), BNI increased burst duration (e.g., Fig. 5A). Before administration of BNI (pre-BNI) the distribution of burst durations was highly skewed ( $P < 0.0001$ , Kolmogorov–Smirnov normality test), and only 15.6% of durations were shorter than the mode (15–20 s, mean  $38.6 \pm 3.9$  s, median 26.6 s,  $n = 147$  bursts from six cells). The tail of the histogram was fit well by a single negative exponential decay ( $R^2 = 0.93$ ,  $P < 0.001$ , Fig. 5B):  $f(t) = 61.414 \exp(-0.053t)$ , where  $t =$  time (burst duration). In the presence of BNI, the burst duration had two modes, at 15–20 s and at 50–55 s (mean  $80.8 \pm 12.2$  s, median 51.3 s,  $n = 63$  bursts from six cells,  $P < 0.001$  compared with pre-BNI, Mann–Whitney rank sum test), with 1.6% of bursts shorter than the first mode and 47.6% of bursts shorter than the second mode. The tail of the histogram was fit by a single exponential decay in the presence of BNI ( $R^2 = 0.38$ ,  $P = 0.02$ , Fig. 5B):  $f(t) = 7.984 \exp(-0.021t)$ .

Before BNI administration, the hazard function of burst duration ( $t$ ) was fit by a single exponential rise to a maximum ( $R^2 = 0.97$ ,  $P < 0.001$ , Fig. 5C):  $f(t) = 0.411 [1 - \exp(-0.101t)] - 0.121$ . By contrast to pre-BNI, in the presence of BNI, the hazard function of burst duration was poorly fit by a single exponential rise to maximum ( $R^2 = 0.67$ ,  $P = 0.19$ , Fig. 5C):  $f(t) = 0.221 [1 - \exp(-0.0588t)] - 0.058$ , indicating that when  $\kappa$ -opioid receptors were blocked, the probability of burst termination increased progressively during bursts.

#### *Distributions of interburst intervals during spontaneous activity in vivo*

The distribution of interburst intervals was also highly skewed under basal conditions ( $P < 0.001$ ), and 22.2% of intervals were shorter than the mode (15–20 s, mean  $29.0 \pm 1.1$  s, median 23.6 s). The tail of the histogram was again well fit by a single exponential decay ( $R^2 = 0.96$ ,  $P < 0.001$ , Fig. 4D):  $f(t) = 20.080 \exp(-0.0498t)$ , where  $t$  is the interburst interval, consistent with the interpretation that burst initiation occurs randomly, but only from 15–20 s after

the end of the previous burst. To determine whether the probability of burst initiation varied with time from the end of the preceding burst, we plotted the hazard function of interburst intervals; under basal conditions, the hazard function of interburst interval duration ( $t$ ) was fit by a single exponential rise to a maximum ( $R^2 = 0.78$ ,  $P = 0.001$ , Fig. 4E):  $f(t) = 0.285 [1 - \exp(-0.044t)] + 0.047$ , indicating that the probability of burst initiation increased over the first 15–20 s of the interburst interval and remained relatively constant thereafter.

Because endogenous  $\kappa$ -opioid receptor activation might contribute to the interburst interval (Roper et al. 2004), we also determined whether the interburst intervals were affected by microdialysis administration of BNI in six cells. Before BNI administration, the distribution of interburst intervals was highly skewed ( $P < 0.0001$ , Kolmogorov–Smirnov normality test), and only 25.2% of intervals were shorter than the mode (15–20 s, mean  $23.6 \pm 1.4$  s, median 19.5 s,  $n = 147$  intervals from six cells). The tail of the histogram was well fit by a single negative exponential decay ( $R^2 = 0.96$ ,  $P < 0.001$ , Fig. 5D):  $f(t) = 151.484 \exp(-0.0946t)$ , where  $t =$  time (interburst interval). In the presence of BNI, the modal interval was 20–25 s (mean  $23.6 \pm 1.7$  s, median 21.6 s,  $P = 0.42$  compared with pre-BNI, Mann–Whitney rank sum test), 41.3% of intervals were shorter than the mode, and the interburst interval distribution had a tail that was well fit by a single exponential decay ( $R^2 = 0.61$ ,  $P < 0.001$ , Fig. 5D):  $f(t) = 29.679 \exp(-0.0594t)$ .

Before BNI administration, the hazard function of interburst interval ( $t$ ) was poorly fit by a single exponential rise to a maximum ( $R^2 = 0.61$ ,  $P = 0.24$ , Fig. 5E):  $f(t) = 0.545 [1 - \exp(-0.18t)] - 0.218$ . Similar to pre-BNI, in the presence of BNI, the hazard function of interburst interval was poorly fit by a single exponential rise to maximum ( $R^2 = 0.06$ ,  $P = 0.92$ , Fig. 5E):  $f(t) = 0.212 [1 - \exp(-0.161t)] + 0.0333$ .

#### *Correlation of interburst interval duration with duration of the preceding burst in vivo*

There was a weak negative correlation between burst duration and the duration of the subsequent interburst interval (Pearson product moment correlation coefficient,  $r = -0.12$ ,  $P = 0.04$ ,  $n = 324$  bursts from 28 cells). A similar (but nonsignificant) correlation between burst duration and the subsequent interburst interval was evident before BNI administration ( $r = -0.10$ ,  $P = 0.25$ ,  $n = 147$  bursts from six cells). In the presence of BNI, there was again a significant correlation between burst duration and the subsequent interburst interval ( $r = -0.25$ ,  $P < 0.05$ ,  $n = 63$  bursts from 6 cells).

#### *Distributions of single spikes between bursts in vivo*

We calculated the distributions of the occurrence of single spikes between bursts (in 5-s intervals, measured from the end of the preceding burst) to determine whether the relative refractoriness of burst initiation (suggested by the scarcity of short interburst intervals) reflected a reduced occurrence of spikes or an increased failure of spikes to trigger bursts. Under basal conditions, the distribution of single spikes was fit by a single exponential decay ( $R^2 = 0.90$ ,  $P < 0.001$ ):  $f(t) = 81.472 \exp(-0.035t)$ , where  $t$  is time from the end of the preceding

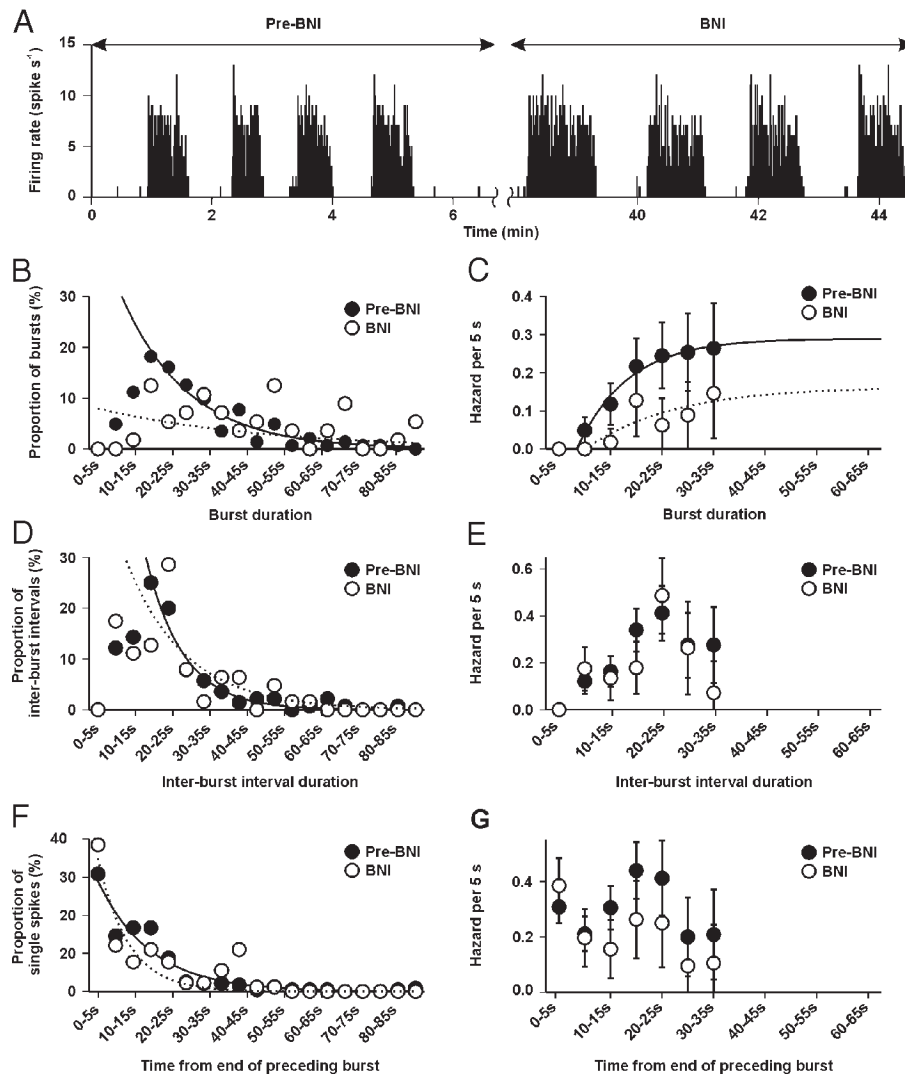


FIG. 5. Effects of endogenous  $\kappa$ -opioid peptides on the distribution of burst duration, interburst intervals, and single spikes between bursts in vivo. **A**: ratemeter record of an extracellular single-unit recording of the firing rate (in 1-s bins) of a spontaneously phasic SON cell in a urethane-anesthetized rat before (pre-BNI) and during (BNI) microdialysis application of BNI into the SON. Note the clear increase in burst duration during BNI administration, typical of all cells tested. **B**: distribution of burst durations under basal conditions (filled circles;  $n = 147$  bursts from six cells); the tail of the histogram is fit by a single exponential decay:  $f(t) = 42.947 \exp(-0.053t)$ , where  $t =$  time (burst duration);  $R^2 = 0.93$ ,  $P < 0.001$ , and distribution of burst durations in the presence of BNI (open circles;  $n = 63$  bursts from six cells); the tail of the histogram was fit by a single exponential decay in the presence of BNI ( $R^2 = 0.38$ ,  $P = 0.02$ ):  $f(t) = 14.258 \exp(-0.021t)$ . **C**: hazard functions generated from the burst distributions in **B** ( $\pm 95\%$  confidence intervals), pre-BNI (filled circles) and in the presence of BNI (open circles); the hazard plots are each fit by single exponential rise to maximum (pre-BNI:  $R^2 = 0.97$ ,  $P < 0.001$ ,  $f(t) = 0.411[1 - \exp(-0.101t)] - 0.121$ ; BNI:  $R^2 = 0.67$ ,  $P = 0.19$ ,  $f(t) = 0.221 [1 - \exp(-0.0588t)] - 0.058$ ). Note that the probability of burst termination increased to a maximum after 20–25 s before BNI administration, but increased progressively with time in the presence of BNI, as well as the separation of some 95% confidence intervals before and during BNI administration. **D**: pre-BNI distribution of interburst intervals (filled circles); the tail of the histogram is fit by a single exponential decay:  $f(t) = 108.203 \exp(-0.0946t)$ , where  $t =$  time (interburst interval);  $R^2 = 0.96$ ,  $P < 0.001$ . The distribution of interburst intervals in the presence of BNI (open circles) was similar to that under basal conditions, and the tail of the histogram was fit by a single exponential decay in the presence of BNI (broken line):  $f(t) = 47.108 \exp(-0.0594t)$ ,  $R^2 = 0.61$ ,  $P < 0.001$ . **E**: hazard functions generated from the interburst interval distributions in **D** ( $\pm 95\%$  confidence intervals), before (filled circles) and during (open circles) BNI administration. **F**: pre-BNI distribution of single spikes between bursts (relative to the end of the preceding burst; filled circles); the histogram is fit by a single exponential decay:  $f(t) = 28.967 \exp(-0.067t)$ , where  $t$  is time (from the end of the previous burst);  $R^2 = 0.92$ ,  $P < 0.001$ . The timing of the occurrence of single spikes between bursts in the presence of BNI (open circles) was similar to that under basal conditions, and the histogram is fit by a single exponential decay in the presence of BNI (broken line):  $f(t) = 34.924 \exp(-0.119t)$ ,  $R^2 = 0.82$ ,  $P < 0.001$ . **G**: hazard functions generated from the single spike distributions in **F** ( $\pm 95\%$  confidence intervals). Note that the regressions plotted above are to the proportions of events, whereas those reported in the text are fitted to the absolute number of events.

burst, consistent with the interpretation that single spikes occur randomly between bursts (Fig. 4F). The hazard function for the distribution of single spikes after the end of bursts revealed that the probability of single spikes occurring was relatively constant throughout the interburst interval (Fig. 4G). Thus the relative refractoriness of burst initiation reflects a reduced

probability that spikes will trigger bursts soon after the end of the preceding burst.

Before BNI administration, the distribution of single spikes was fit by a single exponential decay ( $R^2 = 0.92$ ,  $P < 0.001$ ):  $f(t) = 69.52 \exp(-0.067t)$ , and in the presence of BNI, the timing of the occurrence of single spikes was similar to that

under basal conditions ( $P = 0.97$ , Mann-Whitney rank sum test) and was also fit by a single exponential decay ( $R^2 = 0.82$ ,  $P < 0.001$ ):  $f(t) = 31.911 \exp(-0.119t)$  (Fig. 5F).

## DISCUSSION

Phasic bursts in magnocellular vasopressin MNCs are sustained by activity-dependent plateau potentials that are supported by the summating effects of postspike DAPs. At the beginning of a burst, the DAP is maximal, and DAPs support an initially high firing rate that quickly declines because of spike frequency adaptation, mediated by activation of the medium AHP (Kirkpatrick and Bourque 1996) and the slow AHP (Greffrath et al. 2004). In addition, the DAP mechanism is suppressed, in part because of autocrine inhibition from activity-dependent dynorphin release. Dynorphin is not the only autocrine inhibitory feedback mechanism; adenosine (Noguchi and Yamashita 2000; Oliet and Poulain 1999; Ponzio and Hatton 2005), nitric oxide (Liu et al. 1997; Stern and Ludwig 2001), and vasopressin (Ludwig and Leng 1997) also contribute to activity-dependent depression of vasopressin MNC excitability, as do intrinsic slow after-hyperpolarizing mechanisms (Ghamari-Langroudi and Bourque 2004; Greffrath et al. 1998). Thus in a spontaneous burst, the intraburst firing rate settles to a stable level that reflects a dynamic equilibrium between activity-dependent depolarizing mechanisms (the hyperpolarization-activated inward current (Ghamari-Langroudi and Bourque 2000) and the DAP) and activity-dependent inhibition of excitability. As we show here, the plateau potential, which characterizes this equilibrium, is relatively stable in spontaneous bursts in vitro from the first spike until almost the end of a burst. However, when  $\kappa$ -opioid receptors are blocked, the balance of activity-dependent excitation and inhibition is changed, and as a result, the plateau potential increases progressively during spontaneous bursts and then slowly declines again, apparently reflecting the loss of a rapid feedback inhibition, but unmasking the presence of a slower inhibitory feedback. In our in vitro experiments, two of four cells eventually adopted continuous activity (i.e., ongoing activity was terminated by hyperpolarizing current injection after approximately 2 min of uninterrupted firing) during  $\kappa$ -opioid receptor antagonism, suggesting that (for at least some cells) these slower feedback mechanisms alone are not sufficient to terminate activity. This is consistent with our previous observations that intravenous injection of BNI induces continuous activity in 40% of phasic vasopressin cells in vivo (Brown et al. 1998). Nevertheless, we cannot exclude the possibility that we might have terminated firing prematurely, before these slower mechanisms were able to do so.

We were surprised to find that, on average, a steady-state plateau potential amplitude was attained by the first spike of bursts under basal conditions (Fig. 1D), because summation of consecutive DAPs (Brown 2004) and spike frequency adaptation (Greffrath et al. 2004; Kirkpatrick and Bourque 1996) occur at the beginning of bursts. The apparent rapid rise to steady-state plateau potential seen here might result from the use of a postspike analysis period (100 ms) that precedes the expected time of the DAP peak (200–500 ms after each spike). Indeed hazard analysis of spike timing within bursts in vitro showed that the peak probability of spike firing occurs when the postspike DAP is expected to be maximal (Fig. 2C), and

this might better reflect the influence of the plateau potential on spike timing within bursts. Alternatively, while the plateau potential is probably the principal determinant of burst duration, the dynamic changes in spike timing within bursts could be controlled by more rapid phenomena, such as the velocity of the prespike ramp, which is dictated by the time course of the fast and medium AHPs (Greffrath et al. 2004; Kirkpatrick and Bourque 1996), to which our measure of postspike membrane potential is evidently insensitive.

The observations in vivo show that spontaneous bursts normally last for  $\geq 15$ –20 s, but after about 25 s of firing, the probability of a burst stopping is independent of burst duration; that is, burst termination is a random event after the initial phase of a burst. When  $\kappa$ -opioid receptors are blocked, an inhibitory feedback is removed, allowing the cell to fire faster and resulting in a strengthening of other activity-dependent inhibitory feedbacks. In the presence of BNI, the probability of a burst stopping depends strongly on burst duration, suggesting that these other activity-dependent inhibitory mechanisms strengthen more slowly than feedback mediated by  $\kappa$ -opioid receptors. In the presence of BNI in vitro, the plateau potential amplitude at the end of bursts (as well as the postburst DAP amplitude) is higher than that which sustains activity under basal conditions, indicating that when  $\kappa$ -opioid receptors are blocked, burst termination does not depend simply on plateau potential inhibition. Because synaptic input is essential for firing during phasic bursts in vivo (Brown et al. 2004a), it appears probable that spontaneous EPSPs become progressively less effective at triggering spikes when bursts are prolonged by  $\kappa$ -opioid receptor blockade. Vasopressin reduces EPSP amplitude (Hirasawa et al. 2003; Kombian et al. 2000), increases IPSP frequency (Hermes et al. 2000), and prolongs burst duration, so dendritically released vasopressin might progressively reduce the effectiveness of EPSPs at triggering spikes when  $\kappa$ -opioid receptors are blocked.

The slow AHP has been proposed to terminate bursts (Greffrath et al. 1998), and inhibiting it with muscarinic receptor agonists increases plateau potential amplitude and prolongs spontaneous phasic bursts (Ghamari-Langroudi and Bourque 2004). Thus when  $\kappa$ -opioid receptors are blocked, bursts might be terminated by progressive activation of the slow AHP. Alternatively, or additionally, other factors proposed to be released by vasopressin MNCs such as vasopressin itself (Gouzenes et al. 1998; Hirasawa et al. 2003; Kombian et al. 2000; Ludwig and Leng 1997), apelin (De Mota et al. 2004), galanin (Papas and Bourque 1997), or adenosine (probably generated from ATP released from vasopressin MNCs) (Noguchi and Yamashita 2000; Oliet and Poulain 1999; Ponzio and Hatton 2005) might terminate bursts when  $\kappa$ -opioid receptors are blocked.

### *What keeps vasopressin neurons silent between bursts?*

The silent periods between bursts last for  $\geq 10$  s, but after about 15 s, the probability of a burst starting is independent of the duration of the silent period, and this is unaffected by blocking  $\kappa$ -opioid receptors. Thus like burst termination, the initiation of spontaneous bursts is also governed by apparently random events. It has been proposed that residual dynorphin released during a burst might actively suppress activity on burst termination (Roper et al. 2004), because DAPs recover

from activity-dependent inhibition with a time constant of approximately 5 s (Brown and Bourque 2004), which would allow for full recovery over approximately 10–20 s, the usual range for the duration of interburst intervals *in vivo*. Consistent with this, we found that the postburst DAP is enhanced when  $\kappa$ -opioid receptors are blocked *in vitro*, which would be expected to increase the excitability of cells immediately after each burst. However, the distribution of interburst intervals was not affected by  $\kappa$ -opioid receptor antagonism *in vivo*, nor was that of individual spikes that occasionally occur between bursts. Thus while endogenous dynorphin might suppress activity immediately after a burst (evident as the exposure of a 1-mV increase in the postburst DAP on antagonism of  $\kappa$ -opioid receptors during intracellular recording *in vitro*), it has a negligible contribution to the overall duration of the interburst intervals measured *in vivo*; the marked hyperpolarization on burst termination (approximately 10 mV), along with the relaxation of this hyperpolarization, appears a more important determinant of the interburst interval than inhibition of the DAP. It seems that the recovery of the DAP from active  $\kappa$ -opioid inhibition simply resets the mechanism for activation of the following burst, rather than appreciably suppressing activity between bursts.

The duration of the silent period between bursts was correlated with the duration of the preceding burst, suggesting that an activity-dependent mechanism contributes to the duration of the silent period; this mechanism does not appear to involve activation of  $\kappa$ -opioid receptors because this correlation persisted in the face of  $\kappa$ -opioid receptor antagonism. *In vivo*, phasic bursts can be evoked in vasopressin MNCs by carotid occlusion, but not if it is applied too soon after the preceding burst (Dreifuss et al. 1976). Similarly, brief trains of applied antidromic spikes can trigger bursts in vasopressin MNCs *in vivo*, but not if they are applied too soon (<approximately 10 s) after the end of a burst (Brown et al. 2004a; Leng et al. 1999). Thus there seem to be mechanisms that actively suppress burst initiation for a short time after each burst. *In vitro*, a slow depolarization brings the membrane potential closer to spike threshold immediately preceding burst onset (Boehmer et al. 2000). This slow depolarization (seen as a relaxation of membrane hyperpolarization following burst termination in Fig. 3A) developed over the course of seconds, suggesting that (presumably in addition to other mechanisms) the slow AHP (time constant approximately 2 s, measured after trains of evoked spikes; Ghamari-Langroudi and Bourque 2004) might actively suppress burst initiation for a short time after each burst. The slow depolarization gradually approached spike threshold over approximately 30 s *in vitro*. If such a time course also occurs *in vivo*, this would progressively increase the probability that DAPs that follow random spikes will sustain further spiking by increasing the chances that ongoing EPSPs will reach threshold to trigger the subsequent burst. Indeed, DAPs are themselves voltage dependent (Bourque 1986) and so will increase in amplitude as the slow depolarization develops over the interburst interval, further increasing the probability of superimposed EPSPs reaching spike threshold. Thus random EPSPs superimposed on the slow depolarization might explain the temporal profile of the distribution of burst initiation observed *in vivo*.

### Concluding remarks

Plateau potentials sustain phasic bursts in MNCs, and we show that these plateau potentials are subject to endogenous autocrine feedback inhibition via  $\kappa$ -opioid receptor activation, which is likely to be a major determinant of the timing of burst termination. By contrast, membrane potential between bursts is largely unaffected by endogenous  $\kappa$ -opioid receptor activation. We further show that the temporal profile of burst durations and interburst intervals *in vivo* is consistent with a strong random influence over the timing of burst initiation and termination. Burst initiation was little influenced by endogenous  $\kappa$ -opioid receptor mechanisms, whereas the timing of burst termination was disrupted by blockade of endogenous  $\kappa$ -opioid receptor mechanisms. Taken together, these observations suggest that dendritic dynorphin release contributes to the termination of spontaneous phasic bursts *in vivo* by autocrine inhibition of plateau potential amplitude, reducing the probability of EPSPs reaching spike threshold to trigger further spike firing as bursts progress.

### ACKNOWLEDGMENTS

We are grateful to Dr. Louise Johnstone for allowing the incorporation of data in the analyses presented in Fig. 4.

### GRANTS

This research was supported by Wellcome Trust Grants 058040 and 070118 to C. H. Brown, The Canadian Institutes of Health Research to C. W. Bourque, The Medical Research Council to G. Leng, The Biotechnology and Biological Sciences Research Council to M. Ludwig and The Otago School of Medical Sciences Strategic Equipment (Bequest) Fund to C. H. Brown.

### REFERENCES

- Andrew RD and Dudek FE. Burst discharge in mammalian neuroendocrine cells involves an intrinsic regenerative mechanism. *Science* 221: 1050–1052, 1983.
- Armstrong WE, Smith BN, and Tian M. Electrophysiological characteristics of immunohistochemically identified rat oxytocin and vasopressin neurones *in vitro*. *J Physiol* 475: 115–128, 1994.
- Boehmer G, Greffrath W, Martin E, and Hermann S. Subthreshold oscillation of the membrane potential in magnocellular neurones of the rat supraoptic nucleus. *J Physiol* 526: 115–128, 2000.
- Bourque CW. Calcium-dependent spike after-current induces burst firing in magnocellular neurosecretory cells. *Neurosci Lett* 70: 204–209, 1986.
- Bourque CW, Randle JC, and Renaud LP. Calcium-dependent potassium conductance in rat supraoptic nucleus neurosecretory neurons. *J Neurophysiol* 54: 1375–1382, 1985.
- Brown CH. Rhythmogenesis in vasopressin cells. *J Neuroendocrinol* 16: 727–739, 2004.
- Brown CH and Bourque CW. Autocrine feedback inhibition of plateau potentials terminates phasic bursts in magnocellular neurosecretory cells of the rat supraoptic nucleus. *J Physiol* 557: 949–960, 2004.
- Brown CH and Bourque CW. Mechanisms of rhythmogenesis: insights from hypothalamic vasopressin neurons. *Trends Neurosci* 29: 108–115, 2006.
- Brown CH, Bull PM, and Bourque CW. Phasic bursts in rat magnocellular neurosecretory cells are not intrinsically regenerative *in vivo*. *Eur J Neurosci* 19: 2977–2983, 2004a.
- Brown CH, Ghamari-Langroudi M, Leng G, and Bourque CW. Kappa-opioid receptor activation inhibits post-spike depolarizing after-potentials in rat supraoptic nucleus neurones *in vitro*. *J Neuroendocrinol* 11: 825–828, 1999.
- Brown CH and Leng G. *In vivo* modulation of post-spike excitability in vasopressin cells by kappa-opioid receptor activation. *J Neuroendocrinol* 12: 711–714, 2000.
- Brown CH, Ludwig M, and Leng G. Kappa-opioid regulation of neuronal activity in the rat supraoptic nucleus *in vivo*. *J Neurosci* 18: 9480–9488, 1998.

- Brown CH, Ludwig M, and Leng G.** Temporal dissociation of the feedback effects of dendritically co-released peptides on rhythmogenesis in vasopressin cells. *Neuroscience* 124: 105–111, 2004b.
- De Mota N, Reaux-Le Goazigo A, El Messari S, Chartrel N, Roesch D, Dujardin C, Kordon C, Vaudry H, Moos F, and Llorens-Cortes C.** Apelin, a potent diuretic neuropeptide counteracting vasopressin actions through inhibition of vasopressin neuron activity and vasopressin release. *Proc Natl Acad Sci USA* 101: 10464–10469, 2004.
- Dreifuss JJ, Harris MC, and Tribollet E.** Excitation of phasically firing hypothalamic supraoptic neurones by carotid occlusion in rats. *J Physiol* 257: 337–354, 1976.
- Ghamari-Langroudi M, and Bourque CW.** Caesium blocks depolarizing after-potentials and phasic firing in rat supraoptic neurones. *J Physiol* 510: 165–175, 1998.
- Ghamari-Langroudi M, and Bourque CW.** Excitatory role of the hyperpolarization-activated inward current in phasic and tonic firing of rat supraoptic neurons. *J Neurosci* 20: 4855–4863, 2000.
- Ghamari-Langroudi M, and Bourque CW.** Muscarinic receptor modulation of slow afterhyperpolarization and phasic firing in rat supraoptic nucleus neurons. *J Neurosci* 24: 7718–7726, 2004.
- Gouzenes L, Desarmenien MG, Hussy N, Richard P, and Moos FC.** Vasopressin regularizes the phasic firing pattern of rat hypothalamic magnocellular vasopressin neurons. *J Neurosci* 18: 1879–1885, 1998.
- Greffrath W, Magerl W, Disque-Kaiser U, Martin E, Reuss S, and Boehmer G.** Contribution of  $Ca^{2+}$ -activated  $K^{+}$  channels to hyperpolarizing after-potentials and discharge pattern in rat supraoptic neurones. *J Neuroendocrinol* 16: 577–588, 2004.
- Greffrath W, Martin E, Reuss S, and Boehmer G.** Components of after-hyperpolarization in magnocellular neurones of the rat supraoptic nucleus *in vitro*. *J Physiol* 513: 493–506, 1998.
- Hermes ML, Ruijter JM, Klop A, Buijs RM, and Renaud LP.** Vasopressin increases GABAergic inhibition of rat hypothalamic paraventricular nucleus neurons *in vitro*. *J Neurophysiol* 83: 705–711, 2000.
- Hirasawa M, Mougnot D, Kozoriz MG, Kombian SB, and Pittman QJ.** Vasopressin differentially modulates non-NMDA receptors in vasopressin and oxytocin neurons in the supraoptic nucleus. *J Neurosci* 23: 4270–4277, 2003.
- Kirkpatrick K and Bourque CW.** Activity dependence and functional role of the apamin-sensitive  $K^{+}$  current in rat supraoptic neurones *in vitro*. *J Physiol* 494: 389–398, 1996.
- Kombian SB, Mougnot D, Hirasawa M, and Pittman QJ.** Vasopressin preferentially depresses excitatory over inhibitory synaptic transmission in the rat supraoptic nucleus *in vitro*. *J Neuroendocrinol* 12: 361–367, 2000.
- Leng G, Brown CH, and Russell JA.** Physiological pathways regulating the activity of magnocellular neurosecretory cells. *Prog Neurobiol* 57: 625–655, 1999.
- Li Z, Decavel C, and Hatton GI.** Calbindin-D28k: role in determining intrinsically generated firing patterns in rat supraoptic neurones. *J Physiol* 488: 601–608, 1995.
- Li Z and Hatton GI.**  $Ca^{2+}$  release from internal stores: role in generating depolarizing after-potentials in rat supraoptic neurones. *J Physiol* 498: 339–350, 1997.
- Lincoln DW and Wakerley JB.** Electrophysiological evidence for the activation of supraoptic neurones during the release of oxytocin. *J Physiol* 242: 533–554, 1974.
- Liu QS, Jia YS, and Ju G.** Nitric oxide inhibits neuronal activity in the supraoptic nucleus of the rat hypothalamic slices. *Brain Res Bull* 43: 121–125, 1997.
- Ludwig M and Leng G.** Autoinhibition of supraoptic nucleus vasopressin neurons *in vivo*: a combined retrodialysis/electrophysiological study in rats. *Eur J Neurosci* 9: 2532–2540, 1997.
- Noguchi J and Yamashita H.** Adenosine inhibits voltage-dependent  $Ca^{2+}$  currents in rat dissociated supraoptic neurones via A1 receptors. *J Physiol* 526: 313–326, 2000.
- Oliet SH and Poulain DA.** Adenosine-induced presynaptic inhibition of IPSCs and EPSCs in rat hypothalamic supraoptic nucleus neurones. *J Physiol* 520: 815–825, 1999.
- Papas S and Bourque CW.** Galanin inhibits continuous and phasic firing in rat hypothalamic magnocellular neurosecretory cells. *J Neurosci* 17: 6048–6056, 1997.
- Ponzio TA and Hatton GI.** Adenosine postsynaptically modulates supraoptic neuronal excitability. *J Neurophysiol* 93: 535–547, 2005.
- Pow DV and Morris JF.** Dendrites of hypothalamic magnocellular neurons release neurohypophysial peptides by exocytosis. *Neuroscience* 32: 435–439, 1989.
- Renaud LP and Bourque CW.** Neurophysiology and neuropharmacology of hypothalamic magnocellular neurons secreting vasopressin and oxytocin. *Prog Neurobiol* 36: 131–169, 1991.
- Roper P, Callaway J, and Armstrong W.** Burst initiation and termination in phasic vasopressin cells of the rat supraoptic nucleus: a combined mathematical, electrical, and calcium fluorescence study. *J Neurosci* 24: 4818–4831, 2004.
- Sabatier N, Brown CH, Ludwig M, and Leng G.** Phasic spike patterning in rat supraoptic neurones *in vivo* and *in vitro*. *J Physiol* 558: 161–180, 2004.
- Shuster SJ, Riedl M, Li X, Vulchanova L, and Elde R.** The kappa opioid receptor and dynorphin co-localize in vasopressin magnocellular neurosecretory neurons in guinea-pig hypothalamus. *Neuroscience* 96: 373–383, 2000.
- Stern JE and Ludwig M.** NO inhibits supraoptic oxytocin and vasopressin neurons via activation of GABAergic synaptic inputs. *Am J Physiol* 280: R1815–R1822, 2001.